

Network biomarkers of schizophrenia by graph theoretical investigations of Brain Functional Networks

Megha Singh and Ganesh Bagler*

Center for Biologically Inspired System Science, Indian Institute of Technology Jodhpur, Rajasthan, India.

arXiv:1602.01191v1 [q-bio.QM] 3 Feb 2016

Abstract—Brain Functional Networks (BFNs), graph theoretical models of brain activity data, provide a systems perspective of complex functional connectivity within the brain. Neurological disorders are known to have basis in abnormal functional activities, that could be captured in terms of network markers. Schizophrenia is a pathological condition characterized with altered brain functional state. We created weighted and binary BFN models of schizophrenia patients as well as healthy subjects starting from fMRI data in an effort to search for network biomarkers of the disease. We investigated 45 topological features of BFNs and their 27325 higher order combinations (pairs, triads and tetrads). We find that network features embodying closeness, betweenness, assortativity and edge density emerge as key markers of schizophrenia. Also, features derived from weighted BFNs were observed to be more effective in disease classification as compared to those from binary BFNs. These topological markers provide insights into mechanisms of functional activity underlying disease phenotype and could further be used for designing algorithms for clinical diagnosis of schizophrenia as well as its early detection. Thus results from our study could be leveraged for effective treatment of schizophrenia at reduced cost.

Index Terms—Brain functional networks (BFNs), fMRI, network features, schizophrenia.

I. INTRODUCTION

NEURONAL disorders are known to have basis in abnormal brain functional activities. Brain imaging data have been used to investigate underlying structure and function of a healthy brain and also to pin down differences in functional activity under pathological conditions such as schizophrenia, Alzheimers and autism. Beyond identification of neuronal correlates of these disorders, the need to identify patterns in functional activity has paved way for systems modeling of brain activity data and search for higher order features.

Amongst several neuro-imaging techniques, fMRI has gained widespread popularity for scrutinizing brain activity, owing to its high spatial and temporal resolutions. fMRI is a blood oxygen level signal which is indirectly dependent on the neuronal activity. It captures the hemodynamic response function of the brain neuronal activities giving indirect indications of temporal and spatial neuronal changes. The

M. Singh and G. Bagler are with Center for Biologically Inspired System Science, Indian Institute of Technology Jodhpur, Rajasthan, India (email: pg201384008@iitj.ac.in, ganesh.bagler@gmail.com)

G. Bagler is with Dhirubhai Ambani Institute of Information and Communication Technology, Gandhinagar, Gujarat, India (email: ganesh_bagler@daiict.ac.in)

fMRI data is collected in terms of voxels where each voxel corresponds to hemodynamic response of the neural activity. This four-dimensional spatio-temporal fMRI data could be used to create systems-level models of brain activities using graph theoretic (complex networks) approach [1]–[3].

Brain functional networks (BFNs) are graph theoretical models of functional activities that provide a deep visual insight into connectivity patterns within the brain. BFNs could be utilized to measure anatomical or functional connectivity between different brain regions and hence to probe network characteristics of functional connectivity under brain disorders with the help of graph theoretical metrics. There is a growing interest in application of BFN models for studying various cognitive states as well as pathological conditions and development of methods for the same. In last decade, several advances have happened towards application of network theory for investigation of fMRI data [4]. This approach has been used to understand the organization of brain at macro-level using BFN models [5]–[7]. A variety of network modelling approaches have been implemented for this purpose [8], [9]. These studies have provided insights into the systems architecture of the brain and have highlighted salient features such as presence of default mode network in resting state of brain [10], small-world architecture [11], [12], modularity and hierarchical organization [13]–[15].

Significant structural and functional neuronal abnormalities are known to happen under pathological conditions such as schizophrenia [16]–[18], autism [19], [20], and Alzheimers [21]. There is an increased focus in finding potential network biomarkers for brain disorders. This will not only assist clinical diagnosis but could eventually help in early diagnosis and effective treatment at reduced cost.

Schizophrenia, known for altered functional brain state, has been studied with the help of BFN models and machine learning techniques for its classification from healthy brain states. Anderson *et al.* [22] classified schizophrenia patients from healthy under resting and tasked activities using distance matrices modeled from ICAs of fMRI scans with classification accuracies up to 90%. Yang *et al.* [23] demonstrated hybrid machine learning method using fMRI and genetic data of schizophrenic patients for their classification with high accuracies. Similar studies were performed using features extracted from default mode network and motor temporal ICA components employing two level feature detection technique [24]. Using linear and non-linear discriminative methods, Arbabi-

TABLE I
DEMOGRAPHIC PROFILE OF SUBJECTS IN COBRE DATASET.

Parameter	Healthy Subjects	Schizophrenic Patients
Age	35.82±11.58	38.16±13.89
Female (%)	31	19
Right Handedness (%)	96	83

rani *et al.* [25] examined resting state functional connectivity features for disease classification to achieve up to 96% accuracy using non-linear classifiers. Multiple kernel learning was further used by Castro *et al.* [26] to modify the feature selection method thereby achieving improved accuracies. Chyzyk *et al.* [27] used extreme learning machines to build a computer aided diagnostic system employing features derived from fMRI data. Beyond these key studies, many efforts have gone into application of machine learning techniques on fMRI derived brain network parameters for classification of schizophrenia with higher accuracy [28]–[33].

In this study we investigated BFNs constructed from fMRI data of schizophrenia subjects and healthy subjects so as to identify higher order topological features that characterize the disease. Starting with COBRE data set, we implemented the protocol established by Anderson and Cohen [22] for creating BFN models and for their graph theoretical investigations. Towards identification of key distinguishing network features of schizophrenia, we exhaustively investigated 17 and 28 first order derived network features of binary (unweighted) and weighted BFNs, as well as their higher (second, third and fourth) order tuples. We believe that features thus identified could be effectively used for semi-automated diagnosis of schizophrenia, and may further be used for early detection protocol.

II. MATERIALS AND METHODS

For investigating systems-level differences in brain activity of healthy subjects and pre-diagnosed schizophrenic patients we used the COBRE dataset. This dataset, obtained from International Neuroimaging Data-Sharing Initiative under 1000 Functional Connectomes Project, comprised of fMRI data of 74 healthy subjects (controls) and 72 patients of schizophrenia with varying ages ranging from 18 to 65 years in both classes. The patients were pre-diagnosed with schizophrenia based on ‘structured clinical interview’ used for DSM disorders. Echo-planar imaging was used for resting state fMRI data collection with (Repetition Time) TR=2s, (Echo Time) TE=29ms, matrix size: 64×64, slices=32, voxel size=3×3×4 mm³. Table I depicts the demographic profile of the subjects. Detailed profiles of all subjects are provided in Table S1 of Supplementary Material.

The fMRI data is a 4-Dimensional metadata comprising of information from spatial and temporal dimensions of blood oxygen-level dependent activities under resting state of the brain, along with some additional information about the dataset such as its size, dimensions and details of voxels. We implemented a protocol for transforming fMRI data into their functional network representation described by Anderson and Cohen [22]. This protocol involves a series of steps

including pre-processing of the raw fMRI data, decomposing 4-D data into spatial and time series components using ICA, creating functional graphs from the components thus extracted, and finally evaluating graph theoretical properties of brain functional networks. Following are details of each of these steps of the protocol implemented.

A. Preprocessing

The COBRE data needs to be processed before further analysis. The preprocessing step is aimed at removal of artifacts and standardizing locations of brain regions across all subjects. As a first step of pre-processing, motion correction was implemented for each subject by synchronizing signals recorded in each voxel across all slices. This step corrects any misrepresentation of data from individual voxels due to subject’s head motion. The corrected recording from each voxel was obtained by shifting images from each slice with respect to the reference image. This step was then followed by filtering steps, which include spatial and temporal filtering as well as noise reduction. We obtained filtered 4-D fMRI data for each subject at the end of pre-processing steps, which were performed using fMRI Software Library (FSL) [34].

B. Independent Component Analysis (ICA)

Extracting meaningful features from this high dimensional fMRI data is expected to reduce the redundancy and noise that is not removed at the pre-processing stage. Towards this end ICA was implemented to bring down the complexity of this high dimensional data to a manageable level [35], [36]. The four dimensional space-time fMRI data was represented in terms of an array of dimension (T, X * Y * Z) such that the fMRI scan of time length T and space S can be represented by a linear combination of M < T components and corresponding time series:

$$X_{ts} = \sum_{\mu=1}^M A_{t\mu} C_{\mu s} \quad (1)$$

where X_{ts} represents raw scan intensity at time t and space point s, $A_{t\mu}$ is the amplitude of component μ at time t, $C_{\mu s}$ is the magnitude of component μ at space point s and M stands for total number of components. For the COBRE data the time points T in the signal were 150 and X, Y and Z were 64, 64 and 32 where X and Y are number of points in two dimensional space and Z is the slice number.

In ICA, data is assumed to be a linear combination of signals and fMRI data complies with this assumption. Spatial ICA was employed to decompose fMRI data into a set of maximally spatially independent maps and their corresponding time-courses. These time-courses show considerable amount of time-dependencies between distinct functional activities captured in various components, indicating their potential for use in functional network connectivity analysis. The time-courses, that measure time-varying activity of components, were used for further analysis. These components represent spatially independent time-varying functional activities of the brain under resting state. The ICA of fMRI data was implemented using FSL.

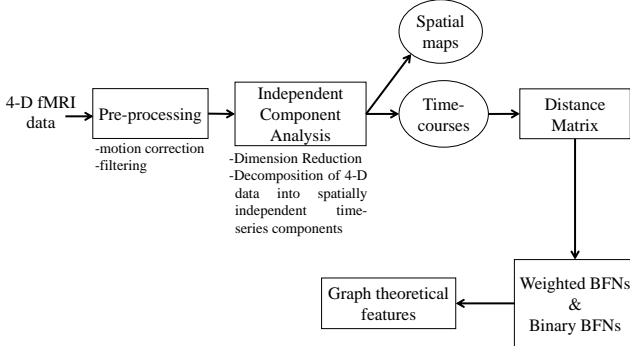


Fig. 1. Strategy implemented for modeling 4-D fMRI data as brain functional network and its topological characterization.

C. Brain Functional Networks and enumeration of network parameters

Brain functional network is a complex networks model of brain where a node represents ‘spatially’ independent functional activity extracted with ICA and an edge specifies the ‘extent’ of temporal dependency between the nodes. Temporal dependencies between functional activities were measured by finding correlations between them. Dependencies were computed using a correlation based distance metric that is a transformation of the maximal absolute cross-correlation between two time-series. For every pair of nodes cross-correlation function (CCF) was calculated over a range of temporal lags,

$$CCF(X_{\mu_i}, X_{\mu_j}, l) = \frac{E[(x_{\mu_i, t+l} - \bar{X}_{\mu_i})(x_{\mu_j, t} - \bar{X}_{\mu_j})]}{\sqrt{E[(x_{\mu_i, t} - \bar{X}_{\mu_i})^2]E[(x_{\mu_j, t} - \bar{X}_{\mu_j})^2]}} \quad (2)$$

where, X_{μ_i} , X_{μ_j} are time series of i^{th} and j^{th} components, l is the temporal lag between them and varied from 0 to 3 points (total 6 seconds with an interval of 2 seconds). The distance matrix $dist(X_{\mu_i}, X_{\mu_j})$ was determined by subtracting maximal absolute CCF from 1 and is given by,

$$d(X_{\mu_i}, X_{\mu_j}) = 1 - max[|CCF(X_{\mu_i}, X_{\mu_j}, l)|] \quad (3)$$

This distance signifies temporal similarity between two components; the higher the distance lesser the correlation. The distance matrix, thus calculated, represents the weighted brain functional network of a subject.

The weighted BFN was further pruned to remove weak connections on the basis of k-nearest neighbor approach where k was chosen as 10% of total components of the subject or 2, whichever was maximum. This pruned BFN was used for computation of graph theoretical parameters. While the graph creation was implemented by R programming language [37], computation of graph theoretical metric was done in MATLAB. Fig. 1 shows the strategy implemented to obtain BFN of each subject and for its graph theoretical characterization.

Binary BFNs were obtained by thresholding the weighted BFNs. The threshold was chosen on trial and error basis such that a single component network is maintained. Following

network parameters were computed on both the binary as well as weighted BFNs for each subject: degree, edge density, node betweenness, edge betweenness, clustering coefficient, characteristic pathlength, efficiency, modularity, closeness, coreness, eccentricity and weak ties. This study was aimed at identification of network parameters that play crucial role in discriminating BFNs of schizophrenia subjects from those of controls. Towards this end we computed higher order statistics (mean, median and standard deviation) for the above mentioned network parameters. We obtained 28 and 17 such statistical features for weighted and binary BFNs, respectively. Table S2 in Supplementary Material provides an exhaustive list of all network derived features.

D. Feature Classification

The BFNs were classified into schizophrenic and control subjects on the basis of the network features derived from weighted as well as binary BFNs. Support Vector Machine (SVM) was used as a classifier with radial basis function as its kernel function. When trained with features of BFNs along with their predefined classes, SVM can classify test cases of BFNs. The performance of SVM classification was assessed with 10-fold cross validation statistics.

We investigated the feature set consisting of individual network features (of weighted and binary BFNs) as well as their pairwise, triad and tetrad combinations with a total of 146 subjects. Combinations with more than four features were not only computationally challenging but were also found to be redundant towards identification of optimal feature set. Our study identified topological features of BFNs with potential for accurate classification between schizophrenia and healthy subjects by an exhaustive search of network features and their higher combinations without using feature selection approach.

III. RESULTS

A. Brain Functional Networks

Brain Functional Networks represent systems model of brain functional activities. Fig. 2 depicts detailed process used for creation of BFNs starting from raw fMRI data. The raw fMRI data was pre-processed to obtain a filtered fMRI signal which was further decomposed into spatially independent components to fetch time-series for each component using ICA. Using time-series data in components, correlation based normalized distance matrix was calculated. This matrix was transformed into weighted and binary adjacency matrices, which represent the network of independent components. Various graph theoretical properties of BFNs were then computed so as to generate a unique feature set to be used for classification (Table S2 of Supplementary Material). The final features set comprised of pairwise, triad and tetrad combinations of individual features derived from both binary as well as weighted BFNs. The classification between healthy and schizophrenic subjects was performed with the help of these features.

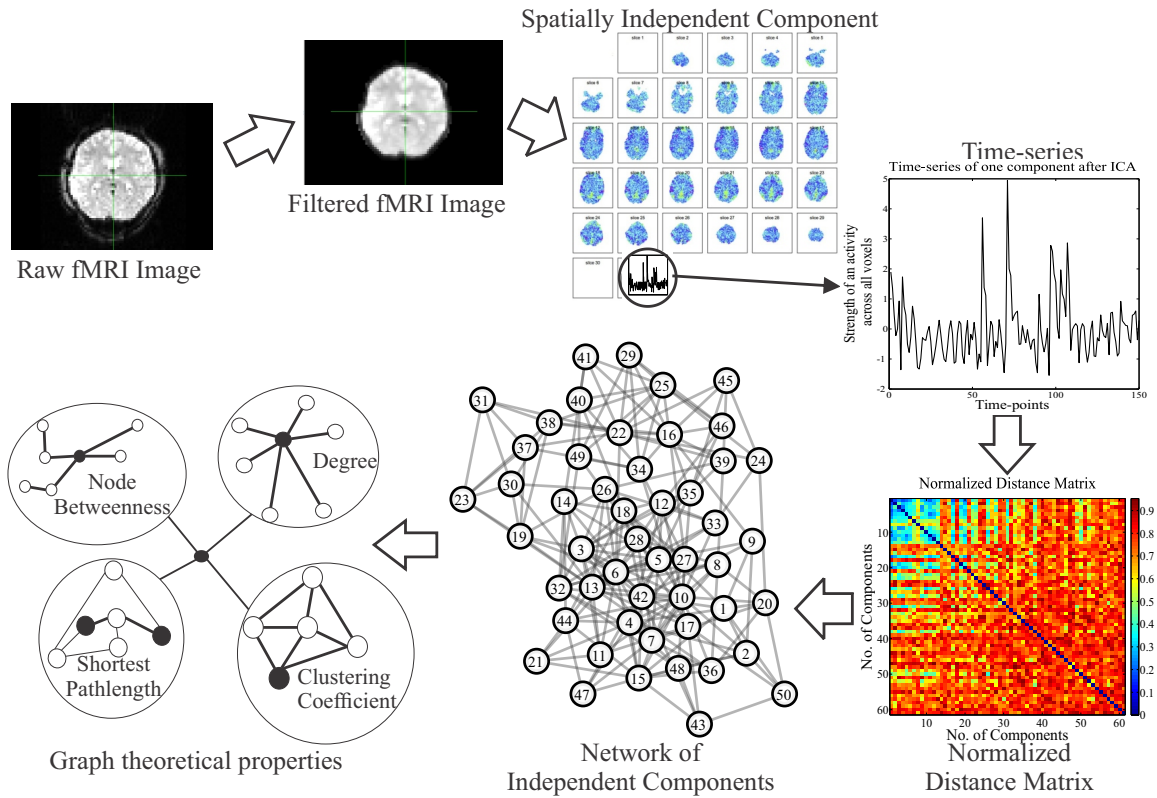


Fig. 2. Detailed procedure implemented for pre-processing of raw fMRI data, creation of brain functional network of independent components and its characterization using graph theoretical metrics.

B. Topological biomarkers of schizophrenia

Towards identification of topological biomarkers of schizophrenia, we investigated network features derived from BFNs of patients and healthy controls. Fig. 3 illustrate apparent differences between (weighted) BFNs and their topological properties of healthy and schizophrenia subjects. The differences that are almost indiscernible at the level of BFN adjacency matrices, become more apparent when seen through the lens of topological features.

Closeness was among the few topological features that contributed significantly to classification accuracy. It reflects proximity of a node to the core of the network. Lower values of closeness represent longer distance to travel between two nodes. The difference in networks belonging to two categories support the hypothesis that recognizes schizophrenia as a disorder of dysfunctional integration between distant brain regions [39], [40]. While the ability to consistently classify schizophrenia BFNs from that of healthy subject may be limited with single features, we anticipated better efficacy for higher order (pairwise, triad and tetrad combinations) features. We present our results on ability to segregate between BFNs of healthy and schizophrenia subjects in the following sections.

C. Individual parameters

First, we created a feature set using individual parameters. For weighted and binary BFNs 28 and 17 such parameters were independently trained and tested in the classifier. Fig. 4 (a) and Fig. 4 (b) show highlights of our studies

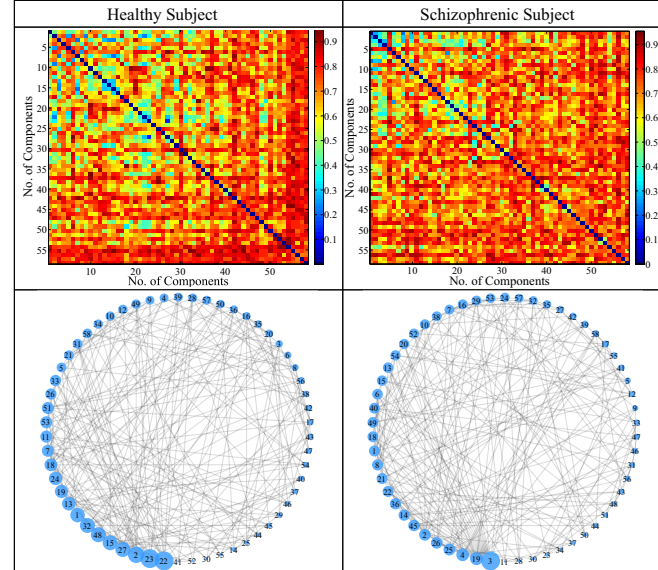


Fig. 3. Normalized distance matrices and their corresponding weighted BFNs for a representative healthy control (40128) and schizophrenic patient (40085). In the distance matrices lighter gray colors represent lower distances thus higher correlation. The weighted BFNs with 58 components (nodes) show nodes sizes scaled to ‘closeness’. The larger the node, higher is its closeness. The networks were visualized using Cytoscape 3.2.0 [38].

with individual parameters with best classification ability (> 55% accuracy; arbitrarily chosen), for weighted and binary BFNs respectively. The accuracy obtained by random sampling

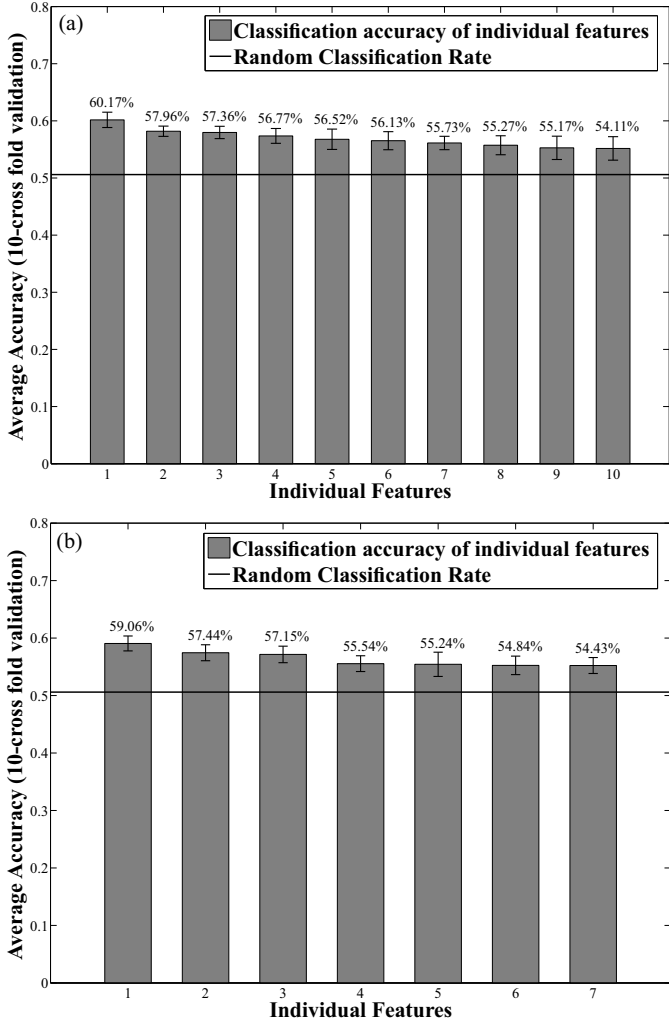


Fig. 4. Average accuracy of best individual network features with their standard errors for (a) weighted, and (b) binary BFNs. Horizontal line shows random classification rate of 50.6%.

stands at 50.6% (shown with a horizontal line in figures) for this dataset. The classification results for all parameters are listed in Table S3 and Table S4 of Supplementary Material. Following were the best individual parameters obtained with weighted BFNs (Fig. 4 (a)): 1. Optimal community structure, 2. Std. deviation of closeness, 3. Longest distance between two vertices, 4. Max. of vertex eccentricity, 5. Sum of product of degrees across all edges, 6. Median closeness, 7. Mean closeness, 8. Median degree, and 9. Maximum degree. Similarly, following were the best individual parameters obtained with binary BFNs (Fig. 4 (b)): 1. Maximum edge overlap, 2. Maximum matching index between two vertices, 3. Number of weak ties, 4. Global efficiency, 5. Edge density, and 6. Maximum edge betweenness.

In weighted networks, the ‘community structure’ underlying the subject’s network provides the best performance individually. On the other hand, the ‘maximum of edge overlap between the two nodes’ in the binary network yielded the highest accuracy.

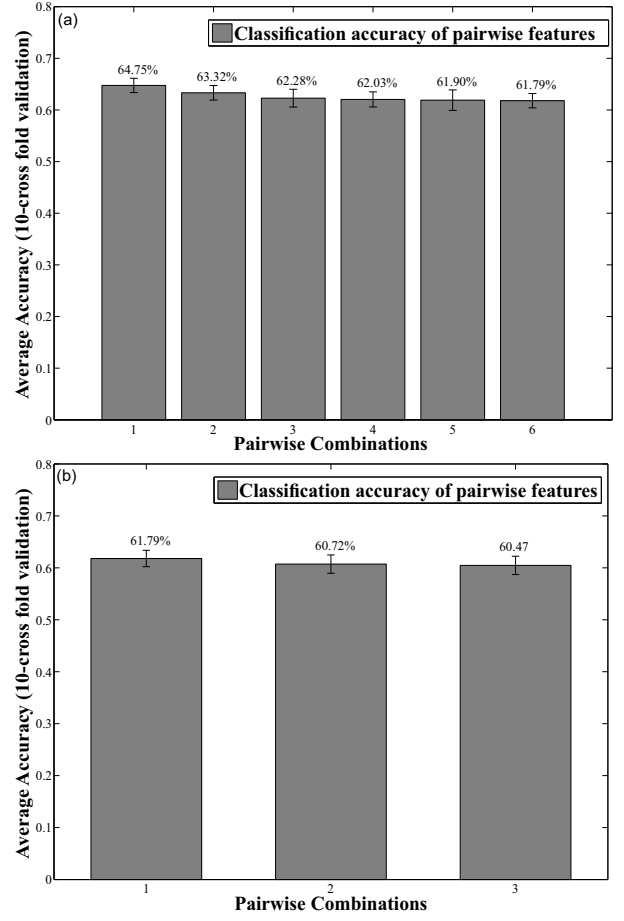


Fig. 5. Average accuracy of top pairwise combinations of network features for (a) weighted and (b) binary BFNs.

D. Pairwise Features

Motivated with the idea of creating a better feature set that could potentially enhance the ability to distinguish between correlations across the BFNs, we created pairwise combination of features set using individual features. The pairwise feature set had 378 and 136 combinations for weighted and binary BFNs, respectively. Interestingly, the classification performance for pairwise features was much better than that of individual features. Fig. 5 (a) and Fig. 5 (b) depict the combinations with accuracies were better than 60% for weighted and binary BFNs, respectively. A more detailed list of top ten pairwise combinations, along with their accuracies and standard deviations, are provided in Table S5 and Table S6 of Supplementary Material.

Optimum community structure emerged as the best feature which when paired with other features yielded among the best classification accuracies. Following were among the best pairwise features (accuracy>60%; chosen arbitrarily) when coupled with ‘optimum community structure’: 1. Std. deviation of closeness, 2. Median closeness, 3. Mean closeness, 4. Assortativity and 6. Max. of vertex eccentricity. Combination 5 in Fig. 5 refers to Characteristic pathlength and Transitivity. Following were the three best pairwise features (accuracy>60%) obtained with binary BFNs (Fig. 5 (b)):

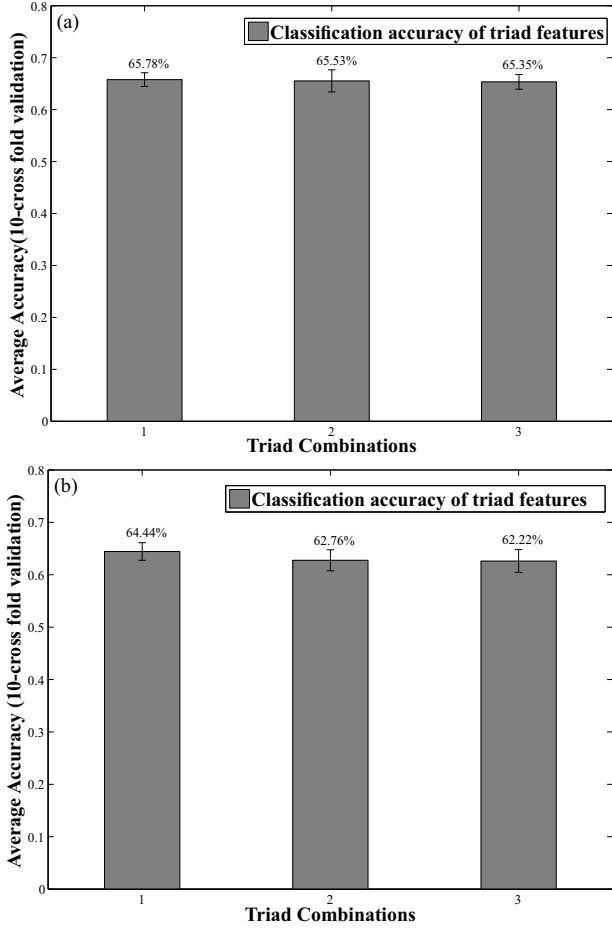


Fig. 6. Average accuracies of top three triad combinations of network features for (a) weighted, (b) binary BFNs.

1. Edge count and Transitivity, 2. Transitivity and Mean closeness and 3. Maximum edge overlap and No. of weak ties. The improved performance of pairwise features compared to that of individual indicates at synergistic effect of multiple topological features extracted from the BFNs leading to better classification accuracy. To test the efficacy of such synergistic effect for higher order of feature combinations, we further created triad features.

E. Triad Features

Creating triad features yields 3276 and 680 such combinations respectively for weighted and binary BFNs. Fig. 6 depicts the classification accuracies of three best triadic features. Detailed results of top ten combinations are provided in Table S7 and Table S8 of Supplementary Material.

The pair ‘Standard deviation of closeness’ and ‘Maximized modularity’ were consistently present among the best three triads of weighted BFNs. When used with 1. Assortativity, 2. Std. deviation of degrees and 3. Maximum matching index, these yielded best classification of schizophrenia BFNs. In binary BFNs, ‘Transitivity’ and ‘Mean closeness’ were consistently present among the best three triadic combinations along with, 1. No. of weak ties, 2. Edge density, and 3. Characteristic

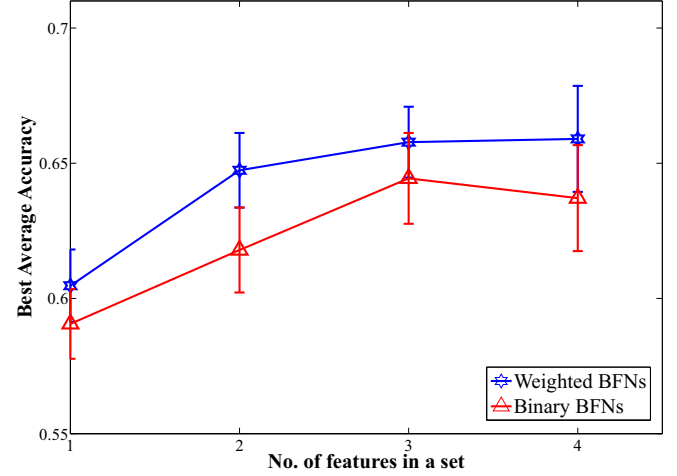


Fig. 7. Best accuracy obtained for classification between BFN models of healthy and schizophrenia brain data with increased order of feature combinations. 1. Individual, 2. Pairwise, 3. Triad and 4. Tetrad features. The error bars represent standard error for 100 experiments of 10-cross fold tests.

pathlength. The improved accuracy with triadic combinations motivated us to examine further higher order combinations.

F. Tetrad Features

We observed that increasing the order of feature combination did not yield any significant improvement above the triads for binary BFNs. Marginal improvement was observed for tetrad features of weighted BFNs. A total of 2380 and 20475 tetrad combinations were investigated for binary and weighted BFNs, respectively. The details of top ten tetrad feature combinations are shown in Table S9 and Table S10 in Supplementary Material.

Fig. 7 summarizes the effectiveness of higher order combinations of network features. The figure shows the trend in highest average accuracy with increasing number of features in the feature set. Improved classification accuracy was observed with increased order of features upto triad combinations. Interestingly, features extracted from weighted BFNs yielded better classification accuracy than those from binary BFNs. With increased complexity of features the accuracy, after initial increase, plateaued. Increased redundancy was observed among the top features obtained.

IV. DISCUSSION

Brain functional networks, graph theoretical models of brain activity data, provide macro-level understanding of complex functional connectivity in the brain [1], [2], [4], [41]. Functional networks of brains in pathological conditions, such as schizophrenia, have been reported to have altered properties quantifiable in terms of topological features (For eg.: low average clustering, long characteristic pathlength, lower degree of connectivity, lower strength of connectivity and reduced modularity) [16], [42]–[45]. Such disruptions of topological features are understood to be an indication of dysfunctionality in schizophrenic BFNs as studied in fMRI scans of dorsal and ventral prefrontal, anterior cingulate, and posterior cortical regions [46], [47].

Here, we performed an exhaustive investigation of graph theoretical features of binary and weighted BFNs and their higher order combinations towards classification of BFNs of schizophrenia and healthy subjects. One of the objectives of our study was to assess the utility of increased order of features on classification accuracy. Other than that we aimed to identify network metrics and their possible implication for altered brain functional patterns.

Our study provides some of the key features that can play an important role in characterizing schizophrenia. Liu *et al.* [16] had shown that small-world organization in brain networks of schizophrenic patients are significantly altered in many brain regions with decreased clustering and increased characteristic path length. Beyond disrupted small world nature, our study presents other properties that may be associated with BFNs of dysfunctional schizophrenic phenotype. Weighted BFNs of schizophrenia subjects were distinct in terms of closeness, sum of product of degrees across all edges, vertex eccentricity, maximized modularity, assortativity and transitivity. On the other hand, binary BFNs presented transitivity, node betweenness, edge density, number of weak ties, characteristic pathlength and matching index between nodes among the best features that could be used for classification of schizophrenia patients from healthy subjects. Broadly these properties reflect on connectivity, modularity and hierarchical organization of the network.

One of the highest accuracies reported with BFN-based models exceeds 65% as reported by Anderson and Cohen [22]. Although, the classification accuracies achieved in our study were not exemplary, our study highlights the role of topological features derived from weighted BFNs for classification of schizophrenia fMRI data. Few key network features (such as closeness, node betweenness, assortativity and edge density) emerged as potential network biomarkers of schizophrenia. The study also underlines limits on higher order feature combinations indicating saturation of classification accuracy. Specific network features obtained from our study could further be used for designing better disease classification algorithms as well as early detection systems.

Our study suggests that instead of exhaustive search for features through higher order combinations of features (n-tuples) appropriate use of feature selection methods could be the way forward. The insights gained from our study into network biomarkers and limitations of higher order features could be used for efficient design of computational protocols for diagnose of schizophrenia at an early stage.

ACKNOWLEDGMENT

GB acknowledges the seed grant support from Indian Institute of Technology Jodhpur (IITJ/SEED/2014/0003) and support from Dhirubhai Ambani Institute of Information and Communication Technology, Gandhinagar. MS thanks the Ministry of Human Resource Development, Government of India as well as Indian Institute of Technology Jodhpur for the Senior Research Fellowship.

REFERENCES

- [1] E. T. Bullmore and D. S. Bassett, "Brain graphs: graphical models of the human brain connectome." *Annual review of clinical psychology*, vol. 7, pp. 113–40, 2011.
- [2] F. De Vico Fallani, D. Bassett, and T. Jiang, "Graph theoretical approaches in brain networks." *Computational and mathematical methods in medicine*, vol. 2012, p. 590483, 2012.
- [3] M. D. Fox, "Clinical applications of resting state functional connectivity," *Frontiers in Systems Neuroscience*, vol. 4, no. June, pp. 1–13, 2012.
- [4] E. Bullmore and O. Sporns, "Complex brain networks: graph theoretical analysis of structural and functional systems." *Nature reviews Neuroscience*, vol. 10, no. 3, pp. 186–98, 2009.
- [5] D. A. Fair, N. U. F. Dosenbach, J. A. Church, A. L. Cohen, S. Brahmbhatt, F. M. Miezin, D. M. Barch, M. E. Raichle, S. E. Petersen, and B. L. Schlaggar, "Development of distinct control networks through segregation and integration." *Proceedings of the National Academy of Sciences of the United States of America*, vol. 104, no. 33, pp. 13 507–12, 2007.
- [6] D. A. Fair, A. L. Cohen, J. D. Power, N. U. F. Dosenbach, J. A. Church, F. M. Miezin, B. L. Schlaggar, and S. E. Petersen, "Functional brain networks develop from a "local to distributed" organization." *PLoS computational biology*, vol. 5, no. 5, pp. 1–14, may 2009.
- [7] J. D. Power, D. A. Fair, B. L. Schlaggar, and S. E. Petersen, "The development of human functional brain networks." *Neuron*, vol. 67, no. 5, pp. 735–48, 2010.
- [8] S. M. Smith, K. L. Miller, G. Salimi-Khorshidi, M. Webster, C. F. Beckmann, T. E. Nichols, J. D. Ramsey, and M. W. Woolrich, "Network modelling methods for fMRI." *NeuroImage*, vol. 54, no. 2, pp. 875–91, 2011.
- [9] M. Kaiser, "A tutorial in connectome analysis: Topological and spatial features of brain networks," *NeuroImage*, vol. 57, no. 3, pp. 892–907, 2011.
- [10] M. D. Greicius, B. Krasnow, A. L. Reiss, and V. Menon, "Functional connectivity in the resting brain: a network analysis of the default mode hypothesis." *Proceedings of the National Academy of Sciences of the United States of America*, vol. 100, no. 1, pp. 253–8, 2003.
- [11] S. Achard, R. Salvador, B. Whitcher, J. Suckling, and E. Bullmore, "A resilient, low-frequency, small-world human brain functional network with highly connected association cortical hubs." *The Journal of neuroscience*, vol. 26, no. 1, pp. 63–72, 2006.
- [12] D. S. Bassett and E. Bullmore, "Small-world brain networks." *The Neuroscientist*, vol. 12, no. 6, pp. 512–23, 2006.
- [13] C. Zhou, L. Zemanová, G. Zamora, C. Hilgetag, and J. Kurths, "Hierarchical organization unveiled by functional connectivity in complex brain networks," *Physical Review Letters*, vol. 97, no. 23, p. 238103, 2006.
- [14] D. Meunier, S. Achard, A. Morcom, and E. Bullmore, "Age-related changes in modular organization of human brain functional networks." *NeuroImage*, vol. 44, no. 3, pp. 715–23, 2009.
- [15] D. Meunier, R. Lambiotte, and E. T. Bullmore, "Modular and hierarchically modular organization of brain networks." *Frontiers in neuroscience*, vol. 4, p. 200, 2010.
- [16] Y. Liu, M. Liang, Y. Zhou, Y. He, Y. Hao, M. Song, C. Yu, H. Liu, Z. Liu, and T. Jiang, "Disrupted small-world networks in schizophrenia." *Brain*, vol. 131, no. Pt 4, pp. 945–61, 2008.
- [17] R. L. Bluhm, J. Miller, R. A. Lanius, E. A. Osuch, K. Boksman, R. W. J. Neufeld, J. Théberge, B. Schaefer, and P. Williamson, "Spontaneous low-frequency fluctuations in the BOLD signal in schizophrenic patients: anomalies in the default network." *Schizophrenia bulletin*, vol. 33, no. 4, pp. 1004–12, 2007.
- [18] Q. Yu, J. Sui, S. Rachakonda, H. He, W. Gruner, G. Pearson, K. A. Kiehl, and V. D. Calhoun, "Altered topological properties of functional network connectivity in schizophrenia during resting state: a small-world brain network study." *PLoS ONE*, vol. 6, no. 9, p. e25423, 2011.
- [19] D. P. Kennedy and E. Courchesne, "The intrinsic functional organization of the brain is altered in autism." *NeuroImage*, vol. 39, no. 4, pp. 1877–85, 2008.
- [20] C. S. Monk, S. J. Peltier, J. L. Wiggins, S.-J. Weng, M. Carrasco, S. Risi, and C. Lord, "Abnormalities of intrinsic functional connectivity in autism spectrum disorders." *NeuroImage*, vol. 47, no. 2, pp. 764–72, 2009.
- [21] C. J. Stam, B. F. Jones, G. Nolte, M. Breakspear, and P. Scheltens, "Small-world networks and functional connectivity in Alzheimer's disease." *Cerebral cortex*, vol. 17, no. 1, pp. 92–9, 2007.

[22] A. Anderson and M. S. Cohen, "Decreased small-world functional network connectivity and clustering across resting state networks in schizophrenia: an fMRI classification tutorial." *Frontiers in human neuroscience*, vol. 7, p. 520, 2013.

[23] H. Yang, J. Liu, J. Sui, G. Pearlson, and V. D. Calhoun, "A hybrid machine learning method for fusing fMRI and genetic data: combining both improves classification of schizophrenia." *Frontiers in human neuroscience*, vol. 4, p. 192, 2010.

[24] W. Du, V. D. Calhoun, H. Li, S. Ma, T. Eichele, K. A. Kiehl, G. D. Pearlson, and T. Adali, "High classification accuracy for schizophrenia with rest and task fMRI data," *Frontiers in Human Neuroscience*, vol. 6, pp. 1–12, 2012.

[25] M. R. Arbabshirani, K. A. Kiehl, G. D. Pearlson, and V. D. Calhoun, "Classification of schizophrenia patients based on resting-state functional network connectivity." *Frontiers in neuroscience*, vol. 7, no. July, p. 133, 2013.

[26] E. Castro, M. R. Arbabshirani, E. Castro, V. D. Calhoun, and I. Fellow, "Accurate classification of schizophrenia patients based on novel resting-state fMRI features resting-state fMRI features," in *Proc. Conf Proc IEEE Eng Med Biol Soc.*, no. July 2015, pp. 6691–6694, 2014.

[27] D. Chyzyk, A. Savio, and M. Graña, "Computer aided diagnosis of schizophrenia on resting state fMRI data by ensembles of ELM," *Neural Networks*, vol. 68, pp. 23–33, 2015.

[28] E. Castro, M. Martínez-Ramón, G. Pearlson, J. Sui, and V. D. Calhoun, "Characterization of groups using composite kernels and multi-source fMRI analysis data: Application to schizophrenia," *NeuroImage*, vol. 58, no. 2, pp. 526–536, 2011.

[29] S. Hayasaka, T. Fekete, M. Wilf, D. Rubin, S. Edelman, R. Malach, and L. R. Mujica-Parodi, "Combining classification with fMRI-derived complex network measures for potential neurodiagnostics," *PLoS ONE*, vol. 8, no. 5, p. e62867, 2013.

[30] R. F. Silva, E. Castro, C. N. Gupta, M. Cetin, M. Arbabshirani, V. K. Potluru, S. M. Plis, and V. D. Calhoun, "The tenth annual MLSP competition: schizophrenia classification challenge the mind research network , 1101 Yale Blvd ., Albuquerque , New Mexico 87106," *IEEE International Workshop on Machine Learning for Signal Processing*, 2014.

[31] A. A. Pouyan and H. Shahamat, "A texture-based method for classification of schizophrenia using fMRI data," *Biocybernetics and Biomedical Engineering*, vol. 35, no. 1, pp. 45–53, 2014.

[32] A. Savio and M. Graña, "Local activity features for computer aided diagnosis of schizophrenia on resting-state fMRI," *Neurocomputing*, vol. 164, pp. 154–161, 2015.

[33] Y. Du, G. D. Pearlson, J. Liu, J. Sui, Q. Yu, H. He, E. Castro, and V. D. Calhoun, "A group ICA based framework for evaluating resting fMRI markers when disease categories are unclear: Application to schizophrenia, bipolar, and schizoaffective disorders." *NeuroImage*, vol. 122, pp. 272–280, 2015.

[34] S. Smith, M. Jenkinson, and M. Woolrich, "Advances in functional and structural MR image analysis and implementation as FSL," *NeuroImage*, vol. 23, pp. S208–S219, 2004.

[35] B. B. Biswal and J. L. Ulmer, "Blind source separation of multiple signal sources of fMRI data sets using independent component analysis." *Journal of computer assisted tomography*, vol. 23, no. 2, pp. 265–71, 1995.

[36] M. J. McKeown, L. K. Hansen, and T. J. Sejnowski, "Independent component analysis of functional MRI: What is signal and what is noise?" *Current Opinion in Neurobiology*, vol. 13, no. 5, pp. 620–629, 2003.

[37] The R Core Team, "R: A language and environment for statistical computing," 2012. [Online]. Available: <http://www.R-project.org/>

[38] P. Shannon, A. Markiel, O. Ozier, N. S. Baliga, J. T. Wang, D. Ramage, N. Amin, B. Schwikowski, and T. Ideker, "Cytoscape : A software environment for integrated models of biomolecular interaction networks," *Genome Research*, pp. 2498–2504, 2003.

[39] E. Bullmore, S. Frangou, and R. Murray, "The dysplastic net hypothesis: an integration of developmental and dysconnectivity theories of schizophrenia," *Schizophrenia Research*, vol. 28, no. 2-3, pp. 143–156, 1997.

[40] K. Friston, "Disconnection and cognitive dysmetria in schizophrenia," *American Journal of Psychiatry*, vol. 162, pp. 429–432, 2005.

[41] M. Rubinov and O. Sporns, "Complex network measures of brain connectivity: uses and interpretations." *NeuroImage*, vol. 52, no. 3, pp. 1059–69, 2010.

[42] D. S. Bassett, E. Bullmore, B. A. Verchinski, V. S. Mattay, D. R. Weinberger, and A. Meyer-Lindenberg, "Hierarchical organization of human cortical networks in health and schizophrenia." *The Journal of neuroscience*, vol. 28, no. 37, pp. 9239–48, 2008.

[43] A. F. Alexander-Bloch, N. Gogtay, D. Meunier, R. Birn, L. Clasen, F. Lalonde, R. Lenroot, J. Giedd, and E. T. Bullmore, "Disrupted modularity and local connectivity of brain functional networks in childhood-onset schizophrenia." *Frontiers in systems neuroscience*, vol. 4, p. 147, 2010.

[44] M.-E. Lynall, D. S. Bassett, R. Kerwin, P. J. McKenna, M. Kitzbichler, U. Muller, and E. Bullmore, "Functional connectivity and brain networks in schizophrenia." *The Journal of neuroscience*, vol. 30, no. 28, pp. 9477–87, 2010.

[45] Q. Yu, S. M. Plis, E. B. Erhardt, E. a. Allen, J. Sui, K. a. Kiehl, G. Pearlson, and V. D. Calhoun, "Modular organization of functional network connectivity in healthy controls and patients with schizophrenia during the resting state." *Frontiers in systems neuroscience*, vol. 5, p. 103, 2011.

[46] I. Ellison-Wright, D. C. Glahn, A. R. Laird, S. M. Thelen, and E. Bullmore, "The anatomy of first-episode and chronic schizophrenia: an anatomical likelihood estimation meta-analysis." *The American journal of psychiatry*, vol. 165, no. 8, pp. 1015–23, 2008.

[47] I. Rish, G. Cecchi, B. Thyreau, B. Thirion, M. Plaze, M. L. Paillere-Martinot, C. Martelli, J.-L. Martinot, and J.-B. Poline, "Schizophrenia as a network disease: disruption of emergent brain function in patients with auditory hallucinations," *PLoS ONE*, vol. 8, no. 1, p. e50625, 2013.

SUPPLEMENTARY MATERIAL

ID	Current Age	Gender	Handedness	Subject Type	Diagnosis
40000	20	Female	Right	Patient	295.9
40001	27	Male	Right	Patient	295.3
40002	19	Male	Right	Patient	295.3
40003	28	Male	Right	Patient	295.1
40004	55	Male	Right	Patient	295.3
40005	48	Female	Right	Patient	295.3
40006	53	Male	Right	Patient	295.6
40007	65	Female	Right	Patient	295.3
40008	28	Male	Right	Patient	295.9
40009	31	Female	Right	Patient	295.3
40010	52	Male	Right	Patient	295.3
40011	28	Male	Left	Patient	295.6
40012	32	Female	Right	Patient	295.3
40013	34	Male	Right	Control	None
40014	31	Male	Right	Control	None
40015	47	Male	Right	Patient	295.3
40016	49	Male	Both	Patient	295.3
40017	30	Female	Right	Control	None
40018	47	Male	Right	Control	None
40019	44	Male	Right	Control	None
40020	22	Male	Right	Control	None
40021	21	Female	Right	Patient	295.3
40022	23	Male	Left	Patient	295.6
40023	48	Male	Right	Control	None
40024	42	Male	Right	Control	None
40025	33	Male	Right	Patient	295.3
40026	44	Male	Right	Control	None
40027	48	Male	Right	Control	None
40028	64	Male	Right	Patient	295.3
40029	20	Male	Right	Patient	295.6
40030	43	Male	Right	Control	None
40031	43	Female	Right	Control	None
40032	31	Female	Right	Patient	295.3
40033	31	Female	Right	Control	None
40034	29	Male	Left	Patient	295.3
40035	30	Male	Right	Control	None
40036	26	Male	Both	Control	None
40037	24	Male	Right	Patient	295.3
40038	53	Female	Right	Control	None
40039	51	Female	Left	Patient	295.7
40040	63	Male	Right	Patient	295.3
40041	62	Male	Right	Patient	295.3
40042	40	Female	Right	Patient	295.3
40043	38	Male	Right	Control	None
40044	48	Male	Left	Patient	290.3
40045	30	Male	Right	Control	None
40046	18	Male	Left	Patient	295.70 depressed type
40047	37	Male	Right	Patient	295.3
40048	31	Male	Right	Control	None
40049	44	Male	Right	Patient	295.3
40050	36	Male	Right	Control	None
40051	23	Male	Right	Control	None
40052	22	Female	Right	Control	None
40053	24	Female	Right	Control	None
40054	52	Male	Right	Control	None

40055	30	Female	Right	Control	None
40056	27	Male	Right	Control	None
40057	36	Male	Right	Control	None
40058	27	Female	Right	Control	None
40059	25	Male	Right	Patient	295.3
40060	41	Male	Right	Patient	295.3
40061	18	Male	Right	Control	None
40062	50	Male	Right	Control	None
40063	37	Male	Right	Control	None
40064	56	Female	Both	Patient	295.6
40065	22	Male	Right	Control	None
40066	62	Male	Left	Control	None
40067	33	Male	Right	Control	None
40068	24	Female	Right	Control	None
40069	58	Male	Right	Control	None
40070	Disenrolled	Disenrolled	Disenrolled	Disenrolled	Disenrolled
40071	51	Female	Right	Patient	295.6
40072	25	Male	Right	Patient	295.3
40073	23	Male	Right	Patient	295.7
40074	34	Female	Right	Control	311
40075	40	Male	Right	Patient	295.1
40076	52	Male	Right	Control	None
40077	28	Male	Right	Patient	295.6
40078	57	Male	Right	Patient	295.6
40079	26	Male	Right	Patient	295.6
40080	26	Male	Right	Patient	295.6
40081	43	Male	Right	Patient	295.7
40082	50	Male	Right	Patient	295.3
40083	Disenrolled	Disenrolled	Disenrolled	Disenrolled	Disenrolled
40084	60	Male	Right	Patient	295.1
40085	22	Male	Right	Patient	295.3
40086	65	Male	Right	Control	None
40087	27	Male	Right	Control	None
40088	33	Female	Right	Patient	295.9
40089	62	Male	Right	Patient	295.3
40090	18	Female	Right	Control	None
40091	24	Male	Right	Control	None
40092	49	Male	Right	Patient	295.3
40093	25	Male	Right	Control	None
40094	57	Male	Left	Patient	295.92
40095	40	Female	Right	Control	None
40096	22	Male	Right	Patient	295.9
40097	52	Female	Right	Patient	296.4
40098	35	Male	Right	Patient	295.3
40099	38	Male	Right	Patient	295.70 bipolar type
40100	35	Male	Right	Patient	295.3
40101	50	Male	Right	Patient	295.3
40102	40	Female	Right	Control	None
40103	40	Male	Right	Patient	295.3
40104	26	Male	Right	Control	None
40105	52	Male	Right	Patient	295.3
40106	46	Male	Right	Patient	295.6
40107	33	Female	Right	Control	None
40108	29	Male	Right	Patient	295.3
40109	33	Male	Right	Patient	295.3
40110	43	Male	Left	Patient	295.7
40111	58	Female	Both	Control	None
40112	42	Male	Right	Patient	295.3

40113	20	Male	Right	Control	None
40114	23	Male	Right	Control	None
40115	27	Male	Right	Control	None
40116	47	Male	Right	Control	None
40117	19	Male	Right	Patient	295.3
40118	34	Female	Right	Control	296.26
40119	44	Female	Right	Control	None
40120	26	Male	Right	Control	None
40121	21	Female	Right	Control	None
40122	22	Male	Right	Patient	295.3
40123	48	Male	Right	Control	None
40124	35	Male	Right	Control	None
40125	48	Male	Right	Control	None
40126	41	Female	Right	Patient	295.3
40127	26	Male	Right	Control	None
40128	22	Male	Right	Control	None
40129	23	Male	Right	Control	None
40130	47	Female	Right	Control	None
40131	47	Male	Right	Control	None
40132	50	Male	Right	Patient	295.7
40133	20	Male	Right	Patient	295.3
40134	42	Male	Right	Control	None
40135	24	Female	Right	Control	None
40136	38	Male	Right	Control	None
40137	21	Male	Left	Patient	295.2
40138	28	Male	Right	Control	None
40139	28	Female	Right	Control	None
40140	53	Female	Right	Control	None
40141	35	Female	Right	Control	None
40142	23	Male	Left	Patient	295.9
40143	52	Male	Right	Patient	295.3
40144	54	Male	Right	Control	None
40145	19	Male	Right	Patient	295.6
40146	39	Male	Right	Control	None
40147	34	Male	Right	Control	None

TABLE S1: Detailed profiles of all subjects.

S.No.	Weighted Network Property	S.No.	Binary Network Property
1.	Node count	1.	Edge count
2.	Minimum degree	2.	Edge density
3.	Maximum degree	3.	Assortativity
4.	Mean degree	4.	Mean node betweenness
5.	Median degree	5.	Maximum node betweenness
6.	Standard deviation of degrees	6.	Standard deviation of node betweenness
7.	Edge density with threshold	7.	Maximum edge betweenness
8.	Assortativity	8.	Longest distance between two vertices
9.	Mean node betweenness	9.	Global efficiency
10.	Maximum node betweenness	10.	Average clustering coefficient
11.	Minimum node betweenness	11.	Transitivity
12.	Standard deviation of node betweenness	12.	Maximum edge overlap
13.	Maximum edge betweenness	13.	Maximum matching index between two vertices
14.	Shortest distance between two vertices	14.	Mean closeness
15.	Global efficiency	15.	Characteristic pathlength
16.	Average clustering coefficient	16.	Number of weak ties
17.	Transitivity	17.	Minimum node betweenness
18.	Optimal community structure		
19.	Maximized modularity		
20.	Maximum of matching index between two vertices		
21.	Median coreness		
22.	Mean closeness		
23.	Median closeness		
24.	Standard deviation of closeness		
25.	Sum of product of degrees across all edges		
26.	Mean Vertex eccentricity		
27.	Standard deviation of node betweenness		
28.	Longest distance between two vertices		

TABLE S2
NETWORK BASED FEATURES OF EACH SUBJECT THAT WERE USED FOR CLASSIFICATION BETWEEN TWO CLASSES.

S.No.	Name of the Parameter	Accuracy	Std. Error
1.	Optimal community structure	60.17	0.0134
2.	Std. deviation of closeness	57.97	0.0108
3.	Longest distance between two vertices	57.36	0.0130
4.	Max. of vertex eccentricity	56.77	0.0178
5.	Sum of product of degrees across all edges	56.53	0.0158
6.	Median closeness	56.13	0.0117
7.	Mean closeness	55.73	0.0166
8.	Median degree	55.27	0.0204
9.	Max. degree	55.17	0.0206
10.	Characteristic pathlength	54.12	0.0213
11.	Global efficiency of the network	53.36	0.0224
12.	Mean degree	52.12	0.0213
13.	Avg. clustering coefficient	51.90	0.0191
14.	Shortest distance between two vertices	51.82	0.0270
15.	Transitivity	51.72	0.0173
16.	Node count	51.68	0.0241
17.	Standard deviation of node betweenness	50.46	0.0222
18.	Max. edge betweenness	50.10	0.0201
19.	Maximized modularity	50.03	0.0192
20.	Median coreness	49.20	0.0244
21.	Minimum degree	49.09	0.0216
22.	Edge density with threshold	49.04	0.0234
23.	Maxi. maximal matching between two vertices	48.18	0.0283
24.	Std. deviation of degrees	47.21	0.0335
25.	Assortativity	45.74	0.0263
26.	Min. node betweenness	44.25	0.0143
27.	Max. node betweenness	41.47	0.0317
28.	Mean node betweenness	41.38	0.0301

TABLE S3
AVERAGE ACCURACIES WITH THEIR STANDARD ERROR FOR ALL BINARY NETWORK PROPERTIES.

S.No.	Name of the Parameter	Accuracy	Std. Error
1.	Maximum edge overlap	59.06	0.0129
2.	Maximum matching index between two vertices	57.44	0.0139
3.	Number of weak ties	57.15	0.0143
4.	Global efficiency	55.54	0.0137
5.	Edge density	55.43	0.0211
6.	Maximum edge betweenness	55.24	0.0161
7.	Minimum node betweenness	55.21	0.0139
8.	Characteristic pathlength	54.84	0.0231
9.	Longest distance between two vertices	54.78	0.0114
10.	Assortativity	54.43	0.0199
11.	Edge count	52.06	0.0163
12.	Mean closeness	50.23	0.0247
13.	Transitivity	49.29	0.0270
14.	Standard deviation of node betweenness	46.93	0.0251
15.	Average clustering coefficient	43.87	0.0284
16.	Maximum node betweenness	42.95	0.0306
17.	Mean node betweenness	42.86	0.0337

TABLE S4
AVERAGE ACCURACIES WITH THEIR STANDARD ERROR FOR ALL BINARY NETWORK PROPERTIES.

S.No.	Name of the Parameter	Accuracy	Std. Error
1.	Optimal community structure & Std. deviation of closeness	64.74	0.0138
2.	Optimal community structure & Median closeness	63.32	0.0140
3.	Optimal community structure & Mean closeness	62.28	0.0171
4.	Optimal community structure & Mean closeness	62.03	0.0146
5.	Characteristic pathlength & Transitivity	61.89	0.0198
6.	Optimal community structure & Max. of vertex eccentricity	61.79	0.0138
7.	Optimal community structure & Max. edge betweenness	60.85	0.0157
8.	Optimal community structure & Sum of product of degrees across all edges	60.62	0.0158
9.	Optimal community structure & Longest distance between two vertices	60.42	0.0141
10.	Optimal community structure & Median degree	60.32	0.0170

TABLE S5
AVERAGE ACCURACIES WITH STANDARD ERROR FOR TOP TEN PAIRWISE COMBINATIONS OF WEIGHTED NETWORK FEATURES.

S.No.	Name of the Parameter	Accuracy	Std. Error
1.	Edge Count & Transitivity	61.79	0.0157
2.	Transitivity & Mean closeness	60.71	0.0177
3.	Maximum edge overlap & Number of weak ties	60.46	0.0176
4.	Minimum node betweenness & Mean closeness	59.38	0.0191
5.	Transitivity & Number of weak ties	59.37	0.0177
6.	Maximum matching index between two vertices & Number of weak ties	59.33	0.0184
7.	Longest distance between two vertices & Transitivity	58.52	0.0147
8.	Maximum matching index between two vertices & Mean closeness	57.89	0.0216
9.	Maximum edge overlap & Maximum matching index between two vertices	57.83	0.0223
10.	Minimum node Betweenness & Transitivity	57.66	0.0206

TABLE S6
AVERAGE ACCURACIES WITH STANDARD ERROR FOR TOP TEN PAIRWISE COMBINATIONS OF BINARY NETWORK FEATURES.

S.No.	Name of the Parameter	Accuracy	Std. Error
1.	Std. deviation of closeness, Maximized modularity & Assortativity	65.78	0.0131
2.	Std. deviation of closeness, Maximized modularity & Std. deviation of degrees	65.53	0.0212
3.	Std. deviation of closeness, Maximized modularity & Maxi. Matching index between two vertices	65.34	0.0141
4.	Std. deviation of closeness, Maximized modularity & Max. of vertex eccentricity	64.47	0.0153
5.	Maximized modularity, Median closeness & Assortativity	64.41	0.0148
6.	Std. deviation of closeness, Maximized modularity & Max. degree	64.20	0.0149
7.	Std. deviation of closeness, Maximized modularity & Mean degree	64.19	0.0134
8.	Std. deviation of closeness, Maximized modularity & Optimal community structure	64.08	0.0145
9.	Std. deviation of closeness, Maximized modularity & Global efficiency of the network	64.05	0.0148
10.	Maximized modularity, Mean closeness & Assortativity	64.01	0.0166

TABLE S7
AVERAGE ACCURACIES WITH STANDARD ERROR FOR TOP TEN THREE FEATURE COMBINATIONS OF WEIGHTED NETWORK FEATURES.

S.No.	Name of the Parameter	Accuracy	Std. Error
1.	Transitivity, Number of weak ties & Mean closeness	64.44	0.0168
2.	Transitivity, Mean closeness & Edge density	62.76	0.0200
3.	Transitivity, Mean closeness & Characteristic pathlength	62.62	0.0218
4.	Transitivity, Mean closeness & Edge count	61.96	0.0178
5.	Transitivity, Edge count & Average clustering coefficient	61.82	0.0186
6.	Transitivity, Edge count & Standard deviation of node betweenness	61.56	0.0218
7.	Transitivity, Number of weak ties & Maximum matching index between two vertices	61.32	0.0202
8.	Transitivity, Mean closeness & Minimum node betweenness	61.17	0.0203
9.	Transitivity, Number of weak ties & Standard deviation of node betweenness	61.16	0.0215
10.	Transitivity, Number of weak ties & Edge count	61.07	0.0167

TABLE S8

AVERAGE ACCURACIES WITH STANDARD ERROR FOR TOP TEN THREE FEATURE COMBINATIONS OF BINARY NETWORK FEATURES.

S. No.	Name of the Parameter	Accuracy	Std. Error
1.	Global efficiency, Transitivity, Maximized modularity & Median closeness	65.90	0.0196
2.	Global efficiency, Transitivity, Maximized modularity & Mean closeness	65.51	0.0184
3.	Mean degree, Assortativity, Maximized modularity & Median closeness	65.49	0.0179
4.	Assortativity, Global efficiency, Maximized modularity & Std. deviation of closeness	65.29	0.0160
5.	Mean degree, Maximized modularity, Mean closeness & Assortativity	65.27	0.0171
6.	Assortativity, Median Coreness, Maximized modularity & Median closeness	65.21	0.0185
7.	Node Count, Assortativity, Median closeness & Maximized modularity	65.10	0.0206
8.	Mean node betweenness, Standard deviation of node betweenness, Median closeness & Maximized modularity	64.97	0.0167
9.	Minimum degree, Assortativity, Median closeness & Maximized modularity	64.86	0.0193
10.	Median degree, Maximized modularity, Mean closeness & Assortativity	64.84	0.0182

TABLE S9

AVERAGE ACCURACIES WITH STANDARD ERROR FOR TOP TEN FOUR FEATURE COMBINATIONS OF WEIGHTED NETWORK FEATURES.

S. No.	Name of the Parameter	Accuracy	Std. Error
1.	Transitivity, Characteristic pathlength, Mean node betweenness & Standard deviation of node betweenness	63.71	0.0196
2.	Transitivity, Edge density, Characteristic pathlength & Mean node betweenness	63.64	0.0197
3.	Transitivity, Edge count, Mean closeness & Standard deviation of node betweenness	63.11	0.0229
4.	Transitivity, Mean closeness, Characteristic pathlength & Standard deviation of node betweenness	62.87	0.0208
5.	Edge density, Maximum matching index between two vertices, Characteristic pathlength & Number of weak ties	62.86	0.0188
6.	Transitivity, Edge density, Mean closeness & Standard deviation of node betweenness	62.79	0.0206
7.	Transitivity, Characteristic pathlength, Mean node betweenness & Edge count	62.71	0.0195
8.	Transitivity, Mean closeness, Maximum matching index between two vertices & Number of weak ties	62.32	0.0178
9.	Transitivity, Number of weak ties, Maximum matching index between two vertices & Edge density	62.24	0.0200
10.	Transitivity, Mean closeness, Global efficiency & Standard deviation of node betweenness	62.16	0.0175

TABLE S10

AVERAGE ACCURACIES WITH STANDARD ERROR FOR TOP TEN FOUR FEATURE COMBINATIONS OF BINARY NETWORK FEATURES.